Myocardial dysfunction and neurohumoral activation without remodeling in left ventricle of monocrotaline-induced pulmonary hypertensive rats

André P. Lourenço, Roberto Roncon-Albuquerque, Jr., Carmen Brás-Silva, Bernardo Faria, Joris Wieland, Tiago Henriques-Coelho, Jorge Correia-Pinto and Adelino F. Leite-Moreira

Am J Physiol Heart Circ Physiol 291:H1587-H1594, 2006. First published 5 May 2006;
doi: 10.1152/ajpheart.01004.2005

Am J Physiol Heart Circ Physiol 291: H1587–H1594, 2006.
First published May 5, 2006; doi:10.1152/ajpheart.01004.2005.

Myocardial dysfunction and neurohumoral activation without remodeling in left ventricle of monocrotaline-induced pulmonary hypertensive rats

André P. Lourenço, Roberto Roncon-Albuquerque, Jr., Carmen Brás-Silva, Bernardo Faria, Joris Wieland, Tiago Henriques-Coelho, Jorge Correia-Pinto, and Adelino F. Leite-Moreira

Department of Physiology, Faculty of Medicine, University of Porto, Porto, Portugal

Submitted 20 September 2005; accepted in final form 23 April 2006

Lourenço, André P., Roberto Roncon-Albuquerque, Jr., Carmen Brás-Silva, Bernardo Faria, Joris Wieland, Tiago Henriques-Coelho, Jorge Correia-Pinto, and Adelino F. Leite-Moreira. Myocardial dysfunction and neurohumoral activation without remodeling in left ventricle of monocrotaline-induced pulmonary hypertensive rats. *Am J Physiol Heart Circ Physiol* 291: H1587–H1594, 2006. First published May 5, 2006; doi:10.1152/ajpheart.01004.2005.—In monocrotaline (MCT)-induced pulmonary hypertension (PH), only the right ventricle (RV) endures overload, but both ventricles are exposed to enhanced neuroendocrine stimulation. To assess whether in long-standing PH the left ventricular (LV) myocardium molecular/contractile phenotype can be disturbed, we evaluated myocardial function, histology, and gene expression of autocrine/paracrine systems in rats with severe PH 6 wk after subcutaneous injection of 60 mg/kg MCT. The overloaded RV underwent myocardial hypertrophy ($P < 0.001$) and fibrosis ($P = 0.014$) as well as increased expression of angiotensin-converting enzyme (ACE) (8-fold; $P < 0.001$), endothelin-1 (ET-1) (6-fold; $P < 0.001$), and type B natriuretic peptide (BNP) (15-fold; $P < 0.001$). Despite the similar upregulation of ET-1 (8-fold; $P < 0.001$) and overexpression of ACE (4-fold; $P < 0.001$) without BNP elevation, the nonoverloaded LV myocardium was neither hypertrophic nor fibrotic. LV indexes of contractility ($P < 0.001$) and relaxation ($P = 0.03$) were abnormal, however, and LV muscle strips from MCT-treated compared with sham rats presented negative ($P = 0.003$) force-frequency relationships (FFR). Despite higher ET-1 production, BQ-123 (ET_A antagonist) did not alter LV MCT-treated muscle strip contractility distinctly ($P = 0.005$) from the negative inotropic effect exerted on shams. Chronic daily therapy with 250 mg/kg bosentan (dual endothelin receptor antagonist) after MCT injection not only attenuated RV hypertrophy and local neuroendocrine activation but also completely reverted FFR of LV muscle strips to positive values. In conclusion, the LV myocardium is altered in advanced MCT-induced PH, undergoing neuroendocrine activation and contractile dysfunction in the absence of hypertrophy or fibrosis. Neuroendocrine mediators, particularly ET-1, may participate in this functional deterioration.

gene expression; myocardial contractility; neuroendocrine stimulation; endothelin-1; heart

IN CARDIAC HYPERTROPHY AND FAILURE, the myocardium is subjected to a combination of two key factors: increased biomechanical load and enhanced neuroendocrine stimulation. The understanding of the relative contribution of these two kinds of stimuli as triggers underlying alterations of myocardial phenotype is only now starting to emerge. Models of experimental pulmonary hypertension (PH) are particularly valuable in this respect because although both ventricles are exposed to neuroendocrine stimulation, only the right ventricle (RV) experiences increased biomechanical load (18). The role of overload as a cause of myocardial hypertrophy, molecular remodeling, and dysfunction in the progression to heart failure (HF) has been substantially underscored in these PH experimental models (16, 18, 30, 32), since most of the changes are restricted to the hypertrophied RV. Yet, some modifications also have been identified in the left ventricular (LV) genome and proteome of rats with hypoxia-induced (32) and monocrotaline (MCT)-induced PH (30). Studying the normally loaded LV of PH rats may be very helpful to ascertain the actions of neuroendocrine systems per se. Curiously, neuroendocrine actions have been considerably highlighted in models of experimental PH. Particularly, endothelin-1 (ET-1) contributes to the progression of cardiopulmonary alterations in MCT-induced PH (24), and chronic therapy with either a selective ET_A or a nonselective $ET_{A/B}$ receptor antagonist improves the survival and ameliorates pulmonary blood flow and RV hemodynamics but, interestingly, also reverses dysfunctional LV contractility and relaxation in MCT-treated rats (14).

The present study was undertaken to characterize the molecular and contractile phenotype of the LV myocardium of MCT-treated rats with advanced PH. After hemodynamic evaluation and morphometric characterization of PH rats 6 wk after MCT injection, we assessed in both ventricles histological features such as myocardial fibrosis and myocyte diameters, and we quantified mRNA levels of genes previously implicated in autocrine/paracrine activation during HF progression such as ET-1, angiotensin-converting enzyme (ACE), type B natriuretic peptide (BNP), angiotensinogen, and aldosterone synthase. We further evaluated the contractile phenotype of the LV myocardium of MCT rats in vitro, performing force-frequency relationships (FFR) in LV muscle strips. Because a considerable increase in myocardial ET-1 mRNA levels was observed, we assessed to greater extent both ET-1 myocardial production by immunostaining and its myocardial actions by acutely blocking ET_A receptors with BQ-123 in LV muscle strips and chronically treating MCT-injected rats with the dual endothelin receptor antagonist bosentan.

METHODS

Animal model. Seven-week-old male Wistar rats (Charles-River, Barcelona, Spain) were housed in groups of five per cage with a controlled environment under a 12:12-h light-dark cycle at a room temperature of 22°C. Rats randomly received either a subcutaneous injection of MCT (60 mg/kg; Sigma Chemical, St. Louis, MO) or an

Address for reprint requests and other correspondence: A. F. Leite-Moreira, Serviço de Fisiologia, Faculdade de Medicina da Universidade do Porto, Alameda Professor Hernâni Monteiro, 4200-319 Porto, Portugal (e-mail: amoreira@med.up.pt).

The costs of publication of this article were defrayed in part by the payment of page charges. The article must therefore be hereby marked "*advertisement*" in accordance with 18 U.S.C. Section 1734 solely to indicate this fact.

equal volume of vehicle and were studied 36–40 days (6 wk) after injection. Previously, we (8) observed that rats develop PH and RV hypertrophy, without overt HF, 22–25 days after subcutaneous injection of 60 mg/kg MCT. Knowing that the time elapsed from injection of MCT to the development of severe hypertrophy and HF is strongly dependent on the dose in relation to the age of the animals studied (35), we decided to study rats 6 wk after injection. Because MCT-treated rats consume significantly less food, the amount of chow fed to sham rats was restricted to the quantity consumed by MCT-treated rats during the previous day, to avoid noticeable differences in nutritional state (18). A group of randomly selected MCT-treated rats underwent chronic daily therapy with 250 mg/kg bosentan (kindly provided by Actelion Pharmaceuticals) administered by gavage (25 mg/ml in 5% gum arabic) starting 2 days after MCT injection and ending 48 h before experimentation. Experiments were subjected to the Portuguese law on animal welfare and conform to the *Guide for the Care and Use of Laboratory Animals* (NIH Publication No. 85-23, revised 1996), having been performed at the Faculty of Medicine of the University of Porto (Porto, Portugal), which is a governmental Institution granted to perform animal research.

Hemodynamic assessment. As previously reported (8), animals (MCT treated and sham, $n = 7$ each) were anesthetized with an intraperitoneal injection of pentobarbital sodium (6 mg/100 mg), mechanically ventilated (Harvard Rodent Ventilator model 683), and compensated for per operative fluid losses. The pericardium was widely opened after a median sternotomy was performed. A silk thread was passed around the ascending aorta to transiently occlude it during the experimental protocol. RV and LV pressures were measured with high-fidelity micromanometers (Millar Instruments SPR-407) inserted into the ventricular cavities. LV septal-lateral diameter was assessed with a sonomicrometer amplifier (Triton Electronics, San Diego, CA) after the implantation of ultrasonic crystals in the interventricular septum and epicardial surface of the LV free wall as previously described (3). After stabilization for 15 min, basal RV and LV peak rate of pressure rise (dP/dt_{max}), end-diastolic pressure (EDP), peak systolic pressure (SP), LV end-diastolic dimension (LVEDD), and peak systolic LV isovolumetric pressure (LVP_{iso}) were recorded. Relaxation rate was estimated with the time constant τ by fitting the isovolumetric pressure fall to a monoexponential function, as previously described (20). Parameters were sampled with a frequency of 1,000 Hz. Recordings were made with respiration suspended at end expiration. An ECG lead (II) was recorded throughout. RV and septum plus LV free wall wet weights were determined at the end of the experimental protocol after anesthetic overdose. Transmural LV and RV free wall samples were snap frozen in liquid nitrogen and stored at −80°C for subsequent molecular analyses.

Intact muscle strip preparations. Briefly, rats were anesthetized with intraperitoneal ketamine-xylazine (50 mg/kg and 8 mg/kg, respectively), a left thoracotomy was performed, and beating hearts were quickly excised and immersed in modified Krebs-Ringer (KR) solution containing (in mM) 93 NaCl, 5 KCl, 1 $MgSO_4$, 1.2 KH_2PO_4, 10 glucose, 1.25 $CaCl_2$, 20 $NaHCO_3$, 1 NaH_2PO_4, 20 $NaC_2H_3O_2$, and 5 U/l insulin with cardioplegic 2,3-butanedione monoxime (BDM; 2.5%) equilibrated with 95% O_2-5% CO_2. Thin muscle strips (cross-sectional diameter < 400 μm) were carefully isolated from LV papillary muscles under a dissecting microscope (Leica Wilde M651), mounted vertically in a 10-ml Plexiglas organ bath, and attached to an electromagnetic length-tension transducer (University of Antwerp, Antwerp, Belgium). Twenty minutes later, bathing solutions were replaced by modified KR solution without BDM. Preload was estimated according to muscle dimensions, and electrical stimulation was set 10% above threshold and at a frequency of 0.5 Hz. Muscles were allowed to stabilize, and the experimental protocol was begun once three comparable basal isotonic and isometric contractions were separately recorded with an interval of at least 10 min. Temperature was kept at 35°C and pH at 7.4 throughout the experimental protocol. In one set of LV muscle strips from sham ($n = 9$), MCT ($n = 9$) and MCT + bosentan rats ($n = 8$), isometric FFR were obtained after an initial period of contraction at 0.5 Hz by stepping up the frequency of stimulation at 3-min intervals and sequentially recording five contractions at 1, 2, 3, 4, and 5 Hz. In another set of LV sham ($n = 7$), MCT ($n = 7$), and MCT + bosentan ($n = 6$) muscle strips, the effects of ET_A antagonism were evaluated by recording several isotonic and isometric contractions before and 20–30 min after a concentration of 1 μM of the selective ET_A antagonist BQ-123 (Sigma Chemical) was added to the bath. Developed tension (mN/mm^2) was computed, using software, from the weight and length of the muscle strip by assuming an ellipsoid shape. Muscle maximum cross-sectional diameters measured with a microscope (Leica DM4000B) were similar ($P = 0.15$) in sham (252 ± 24 μm), MCT (280 ± 27 μm), and MCT + bosentan muscle strips (305 ± 41 μm), excluding the possibility that differences in muscle strip dimensions had an impact on contractile function.

Histology and immunohistochemistry. Transverse 4-μm-thick sections of paraffin-embedded, formalin-fixed specimens encompassing the RV, interventricular septum, and LV free wall were stained and photographed with a digital camera (Leica DFC320) in a group of additional sham ($n = 4$) and MCT rats ($n = 4$). The shortest diameter of 50 transversally cut, randomly selected cardiomyocytes from the RV, septum, and LV free wall myocardium was measured with image analyzer software (Leica IM-1000) at the level of the nucleus in hematoxylin-eosin-stained sections. Two independent, blinded observers ranked histological sections stained with Masson's trichrome for collagen as having no fibrosis (*grade 0*); a localized small amount of fibrosis (*grade 1*); mild, patchy fibrosis (*grade 2*); moderate, diffuse fibrosis (*grade 3*); or severe, diffuse fibrosis (*grade 4*). Immunohistochemical staining of ET-1 was performed with a 1:800 dilution of rabbit ET-1 antiserum (T-4050; Peninsula Laboratories) at 4°C for 16 h after initial incubation with 0.3% H_2O_2 and blocking solution (TR-004-HD; Labvision) at room temperature. The sample was then sequentially exposed at room temperature to biotinylated goat anti-rabbit (TR-004-HD; Labvision) for 15 min, to streptavidin peroxidase (TR-004-HD; Labvision) for 15 min, and, finally, to 4% 3,3-diaminobenzidine (TR-004-HD; Labvision) for 10 min. Counterstaining was performed with hematoxylin.

Relative quantification of mRNA. Two-step real-time RT-PCR was performed as previously described (8). Briefly, after total mRNA extraction (no. 74124; Qiagen), standard curves were obtained for each gene correlating ($R \geq 0.98$) the mRNA quantities in graded dilutions of a rat cardiac tissue sample with the respective threshold cycles (second derivative maximum method). Equal amounts of mRNA from every sample underwent three separate two-step real-time RT-PCR experiments for each gene, using SYBR green as marker (no. 204143; Qiagen). GAPDH was used as internal control, because its mRNA levels were similar in the studied groups. Results are relative to the mean obtained for the sham group (set as arbitrary unit) and normalized for GAPDH. Specific PCR primer pairs for the studied genes are presented in Table 1.

Statistical analysis. Data are expressed as means ± SE. Statistical analysis used a two-way ANOVA to compare cardiomyocyte hypertrophy data; a repeated-measures two-way ANOVA followed by Holm-Sidak's method for multiple comparisons was applied to data from FFR in intact muscle strip preparations; and Fisher's exact test was used to evaluate myocardial fibrosis after categories were grouped. One-way ANOVA and Student's *t*-test were used to compare other results as indicated. Statistical significance was set at a two-tailed value of $P < 0.05$.

RESULTS

Rats were studied 6 wk after injection, at which point the mortality was null in sham rats but ~85% in MCT and 50% in MCT + bosentan rats. All MCT rats presented clinical signs of overt HF, namely, lethargy, labored breathing, cachexia, vein

Table 1. *Primers used in mRNA quantification*

Gene	Sequence 5′ → 3′
GAPDH	fw: TGG CCT TCC GTG TTC CTA CCC
	rev: CCG CCT GCT TCA CCA CCT TCT
ET-1	fw: CCA TGC AGA AAG GCG TAA AAG
	rev: CGG GGC TCT GTA GTC AAT GTG
ACE	fw: GCA GGC CAG CAG GGT CCA CTA CAC
	rev: GAC CTC GCC ATT CCG CTG ATT CT
BNP	fw: GGA CCA AGG CCC TAC AAA AGA
	rev: CAG AGC TGG GGA AAG AAG AG
Angiotensinogen	fw: CGG ACA GCA CCC TAT TTT TCA ACA
	rev: GAG GCG CAC TGG GGC TGG AT
Aldosterone synthase	fw: AAT GGC GCT TCA ACC GAC TG
	rev: GAG CAT TCT GAC GCA CCT TCT TTT
HIF-1α	fw: CTA ACA AGC CGG GGG AGG AC
	rev: TCA TAG GCG GTT TCT TGT AGC

GAPDH, glyceraldehyde-3-phosphate dehydrogenase; ET-1, endothelin-1; ACE, angiotensin-converting enzyme; BNP, type-B natriuretic peptide; HIF-1α, hypoxia-inducible factor-1α.

and liver engorgement, pleural effusion, and ascites. Although MCT + bosentan rats also presented these clinical signs, they distinguished themselves from MCT rats because they showed less lethargy on a qualitative evaluation. The body weight (BW) of sham rats was similar to the BW of MCT and MCT + bosentan rats (266 ± 16, 240 ± 13, and 250 ± 12 g, respectively; $P = 0.37$).

Cardiac hemodynamics, morphometry, and histology. The hemodynamic features of the experimental groups are summarized in Table 2. MCT rats showed a marked increase in RVSP compared with sham rats ($P < 0.001$). This was accompanied by other modifications in hemodynamic profile, such as increased values of RV dP/dt_{max} ($P = 0.014$), τ ($P < 0.001$), and RVEDP ($P = 0.003$), but also by morphometric (Fig. 1) and histological changes (Table 3 and Figs. 1*C* and 2), such as increased ratio of RV weight to BW ($P < 0.001$), increased RV cardiomyocyte diameters ($P < 0.001$), and significantly higher grades of myocardial fibrosis ($P = 0.014$). In contrast to the

Table 2. *Hemodynamic data*

	Sham	MCT
n	7	7
	RV	
RVSP, mmHg	20.8±1.3	51.4±4.1*
RVEDP, mmHg	0.9±0.4	3.9±0.7*
dP/dt_{max}, mmHg/s	936±72	1,411±173*
τ, ms	7.8±0.7	37.8±2.3*
	LV	
LVSP, mmHg	95.1±2.5	60.2±3.5*
LVEDP, mmHg	6.7±0.6	7.8±0.9
LVEDD, mm	6.4±0.8	5.4±0.8
dP/dt_{max}, mmHg/s	4,749±323	2,205±272*
LVP_{iso}, mmHg	193.1±7.2	131.5±6.6*
τ, ms	21.5±1.7	26.9±2.2*

Values are means ± SE. MCT, monocrotaline-treated rats; RV, right ventricle; RVSP, right ventricular systolic pressure; RVEDP, right ventricular end-diastolic pressure; LV, left ventricle; LVSP, left ventricular systolic pressure; LVEDP, left ventricular end-diastolic pressure; LVEDD, left ventricular end-diastolic dimension; dP/dt_{max}, peak rate of ventricular pressure rise; LVP_{iso}, peak systolic isovolumetric pressure; τ, time constant of isovolumetric relaxation. Comparisons were performed using Student's *t*-test. *$P <$ 0.05 vs. sham.

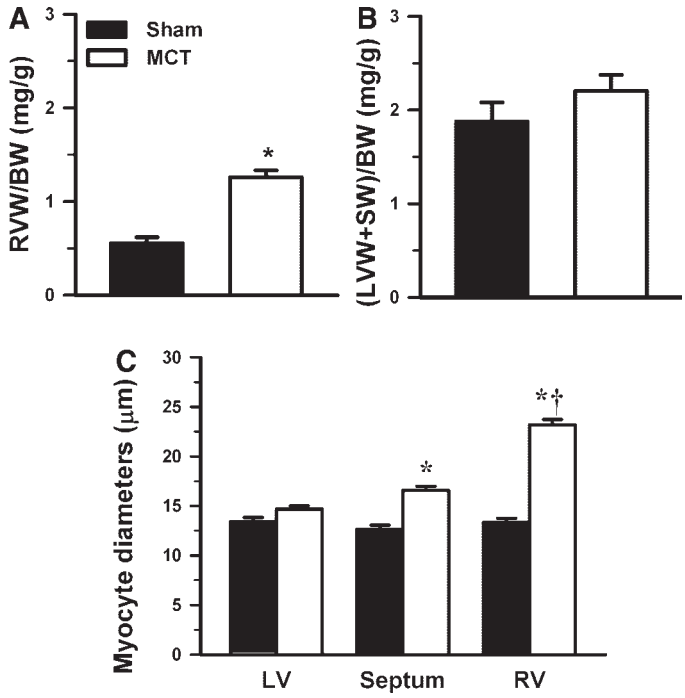

Fig. 1. Hypertrophic response to monocrotaline (MCT)-induced pulmonary hypertension. *A*: right ventricle weight (RVW)-to-body weight (BW) ratio. *B*: left ventricle free wall weight + interventricular septum weight (LVW+SW)-to-BW ratio. Student's *t*-test was used to compare sham ($n = 7$) and MCT-treated rats ($n = 7$). RVW/BW was significantly increased in MCT rats (*$P <$ 0.001). *C*: LV free wall, interventricular septum, and RV free wall cardiomyocyte diameters from sham ($n = 4$) and MCT-treated rats ($n = 4$). Two-way ANOVA and Holm-Sidak's method for multiple comparisons were used in the statistical analysis. Septal cardiomyocytes of MCT-treated rats were significantly larger than cardiomyocytes from sham rats and from the LV of MCT-treated rats (*$P < 0.001$), yet the largest cardiomyocytes were those from the RV of MCT-treated rats, which were significantly larger than the corresponding septal myocytes (†$P < 0.001$).

RV myocardium, the grade of myocardial fibrosis observed in the LV of MCT rats did not differ from that of sham rats (Table 3 and Fig. 2), and despite the tendency toward an increase in the ratio of LV and septum as a whole to BW (Fig. 1), only septal ($P < 0.001$) and not LV free wall cardiomyocytes presented increased diameters (Fig. 1*C*). Likewise, the LV filling pressures as estimated by LVEDP and LVEDD were unaltered. The maximum developed pressures (LVSP), however, were reduced ($P < 0.001$) as well as the indexes of contractility, dP/dt_{max} ($P < 0.001$) and LVP_{iso} ($P < 0.001$),

Table 3. *Myocardial fibrosis*

Fibrosis Grade	Sham		MCT	
	RV	LV	RV	LV
0	3	2	0	1
1	1	2	0	3
2	0	0	3	0
3	0	0	1	0
4	0	0	0	0

Fibrosis grades: 0, no fibrosis; 1, localized small amount of fibrosis; 2, mild patchy fibrosis; 3, moderate, diffuse fibrosis; and 4, severe, diffuse fibrosis. *P* value was calculated using Fisher's exact test after grouping categories (*grades 0* and *1* in sham rat RV vs. *grades 2* and *3* in MCT-treated rat RV). *$P = 0.014$ vs. sham RV ($n = 4$ for sham and MCT).

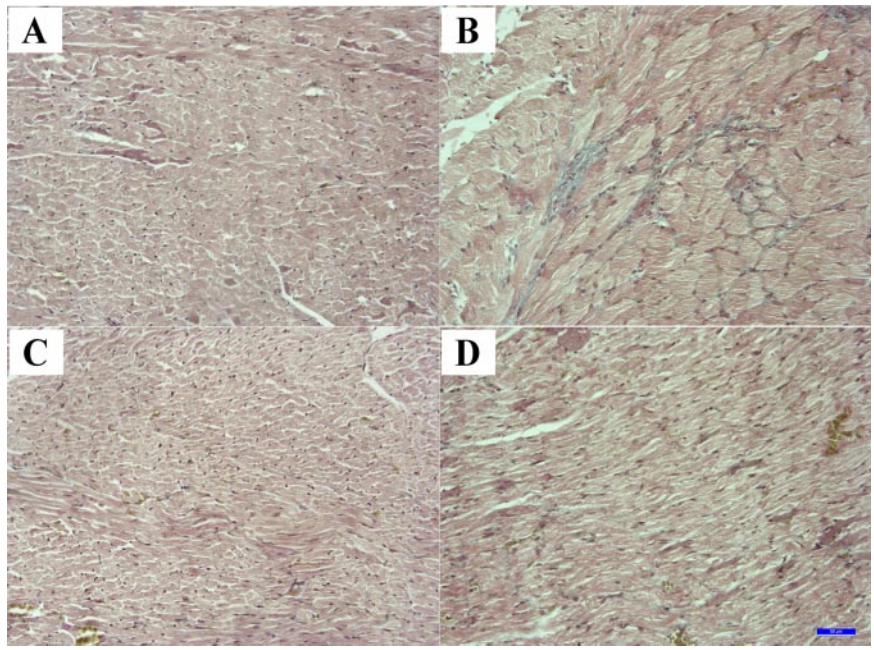

Fig. 2. Representative photomicrographs (×200) of Masson's trichrome-stained sections from sham and MTC-treated rats for evaluation of myocardial fibrosis. *A*: sham rat RV. *B*: MCT-treated rat RV. *C*: sham rat LV. *D*: MCT-treated rat LV. Note the increased fibrosis in the RV of MCT-treated rats.

whereas the relaxation time constant τ was increased ($P = 0.03$) in the LV of MCT rats. The heart rate of MCT rats was significantly decreased as well (sham = 272 ± 14 beats/min vs. MCT = 200 ± 17 beats/min; $P = 0.008$). Chronic therapy with bosentan after MCT injection attenuated RV hypertrophy ($P < 0.001$) as assessed by a reduction in the ratio of RV free wall to LV free wall plus interventricular septum weight (Fig. 3).

Autocrine/paracrine activation. Changes in the expression of genes involved in autocrine/paracrine activation during the progression to heart failure in MCT-treated rats with and without subsequent chronic therapy with bosentan are summarized in Fig. 4. ACE and ET-1 mRNA levels were increased in both the RV and the LV free wall myocardium of MCT rats ($P < 0.01$), whereas BNP mRNA overexpression was restricted to the RV myocardium ($P < 0.001$). The RV myocardium of MCT rats also presented a more pronounced upregulation of the ACE gene ($P = 0.03$), but the increase in ET-1 mRNA levels was not different between ventricles ($P = 0.694$). The indiscriminate increase in ET-1 production was

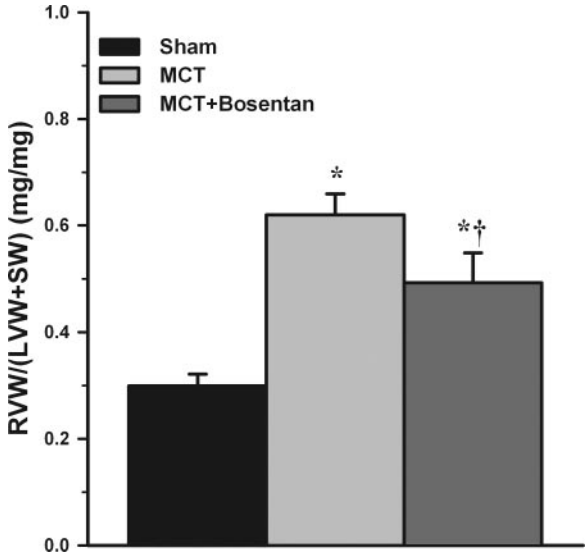

Fig. 3. RVW-to-LVW+SW ratios in sham ($n = 7$) and MCT-treated rats with (MCT+bosentan, $n = 7$) and without subsequent chronic daily therapy with 250 mg/kg bosentan by gavage (MCT, $n = 7$). As evaluated with one-way ANOVA, *$P < 0.001$ vs. sham and †$P < 0.001$ vs. MCT.

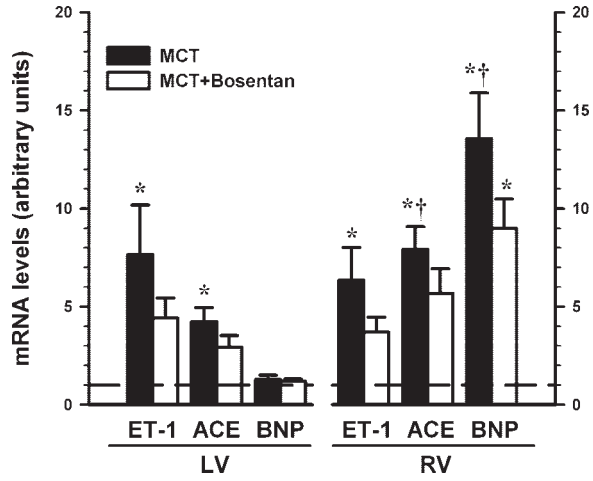

Fig. 4. LV (*left*) and RV (*right*) mRNA levels of angiotensin-converting enzyme (ACE), endothelin-1 (ET-1), and type-B natriuretic peptide (BNP) in rats with MTC-induced pulmonary hypertension with (MCT, $n = 7$) and without chronic daily therapy with 250 mg/kg bosentan by gavage (MCT+bosentan, $n = 7$). Results are expressed as arbitrary units after normalization for GAPDH. The arbitrary unit was set as the average value of the sham group and is presented as a reference line. ACE and ET-1 gene expression were increased in both ventricles of MCT compared with sham ($n = 7$) rats (*$P < 0.01$, as evaluated with one-way ANOVA), whereas MCT+bosentan showed no significant differences in mRNA levels from sham mRNA levels. In MCT and MCT+bosentan, BNP was only overexpressed in the RV (*$P < 0.001$, as evaluated with one-way ANOVA). ACE and BNP were significantly more upregulated in the RV than in the LV of MCT (†$P = 0.03$ and $P = 0.002$ as evaluated with Student's *t*-test, respectively).

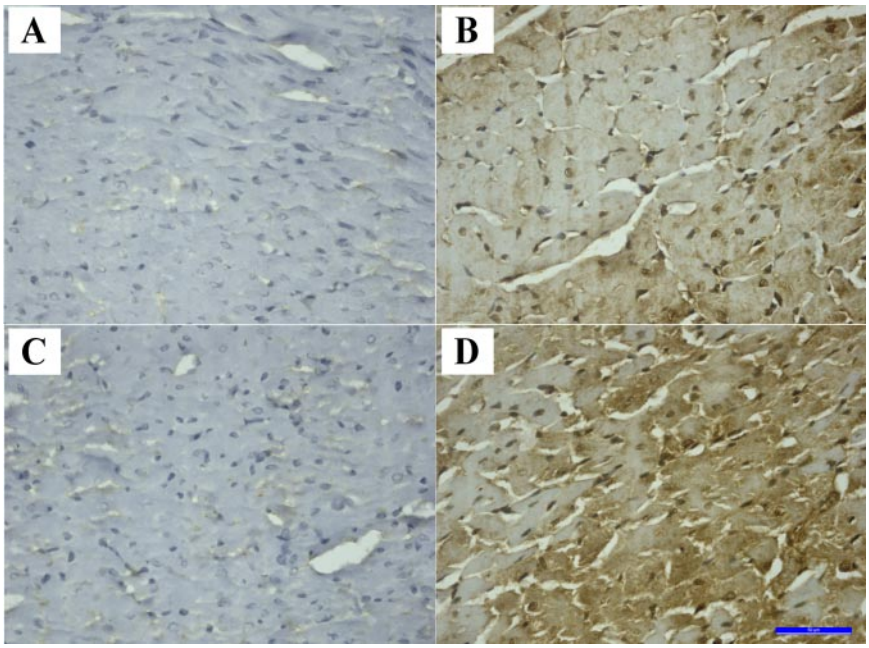

Fig. 5. Representative photomicrographs (×400) showing ET-1 immunohistochemical staining in sham and MCT-treated rat RV and LV free wall myocardium. *A*: sham rat RV. *B*: MCT-treated rat RV. *C*: sham rat LV. *D*: MCT-treated rat LV. ET-1 immunostaining was almost confined to the vascular endothelium in the RV (*A*) and LV (*C*) myocardium of sham rats, whereas in addition to endothelial marking there was also a striking cardiomyocyte staining in the RV (*B*) and LV (*D*) myocardium of MCT-treated rats. Notice as well the cardiomyocyte hypertrophy in the RV myocardium of MCT-treated rats (*B*).

confirmed by a striking immunostaining of cardiomyocytes from both the LV and RV myocardium of MCT rats, whereas the staining in sham rat myocardium was found almost exclusively in vascular endothelium (Fig. 5). The MCT + bosentan group showed no significant differences in the gene expression of ACE and ET-1 in both the RV and the LV compared with either the sham or MCT group, indicating an intermediate level of gene expression (Fig. 4). RV BNP mRNA levels were significantly increased compared with sham rats ($P < 0.001$), and although their increase was of lower magnitude, it did not differ from that of MCT rats.

No significant differences were observed in the RV and LV expression of aldosterone synthase (1.2 ± 0.7 vs. 1.0 ± 0.2, $P = 0.4$, and 1.7 ± 0.8 vs. 1.0 ± 0.2, $P = 0.22$, respectively) or angiotensinogen (1.2 ± 0.3 vs. 1.0 ± 0.1, $P = 0.29$, and 1.3 ± 0.4 vs. 1.0 ± 0.1, $P = 0.22$, respectively) in MCT-treated rats compared with sham rats. The gene expression of transcription factor HIF-1α was studied in the LV of MCT-treated rats to assess a possible role of hypoxia on neuroendocrine activation. No differences were observed (sham = 1.0 ± 0.1 arbitrary units vs. MCT = 1.3 ± 0.2 arbitrary units; $P = 0.22$).

Contractile properties of intact LV muscle strips. Isometrically contracting muscle strips from sham and MCT + bosentan LV showed a steady increase in developed tension between 1 and 5 Hz, indicating positive FFR, whereas MCT LV muscle strips responded in the opposite way ($P < 0.001$), presenting overall negative FFR (Fig. 6). Baseline force development was not different ($P = 0.16$) among the three groups and averaged 2.2 ± 0.4 mN/mm^2. Adding the selective ET_A antagonist BQ-123 to in vitro contracting LV intact muscle strips induced different responses ($P = 0.005$) in sham compared with MCT and MCT + bosentan muscle strips: a negative inotropic effect was elicited in sham muscle strips ($P < 0.032$), whereas the tension developed by MCT and MCT + bosentan muscle strips remained unaltered (Fig. 7).

DISCUSSION

We have demonstrated that the LV myocardium of MCT-treated rats with long-standing PH presents autocrine/paracrine system activation in the absence of a direct hemodynamic stress, and although myocardial hypertrophy and fibrosis are not observed, its contractile phenotype is disturbed.

MCT-treated rats developed PH, RV myocardial hypertrophy, and fibrosis. A higher expression of genes that take part in the processes of molecular remodeling was observed in the chronically overloaded RV myocardium but also in the LV myocardium. Despite the pronounced upregulation of ACE and

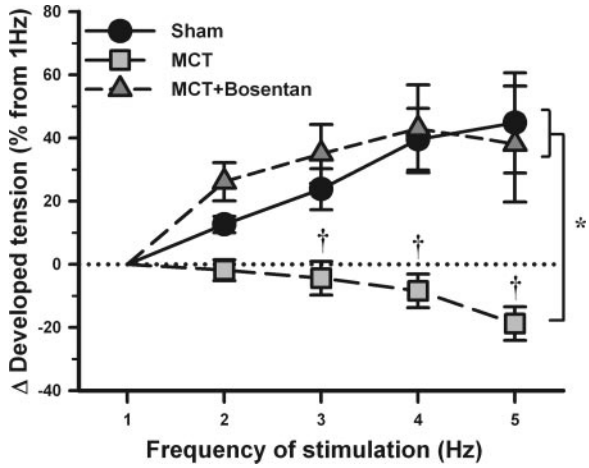

Fig. 6. Force-frequency relationships (FFR) obtained in intact isolated muscle strips from the LV myocardium of sham ($n = 9$), MCT ($n = 9$), and MCT+bosentan rats ($n = 8$). Results are presented as percent variation from baseline (Δ) of developed tension at 1 Hz. Sham and MCT+bosentan LV muscle strips show positive FFR, whereas FFR are negative in MCT LV muscle strips. *$P < 0.001$ for interaction, as evaluated with two-way repeated-measures ANOVA. †$P < 0.001$ vs. sham at an equivalent frequency of stimulation, as evaluated with Holm-Sidak's method for multiple group comparisons.

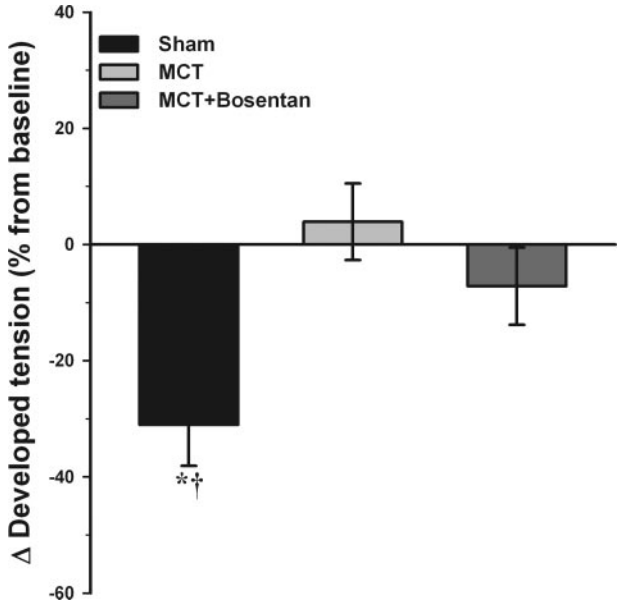

Fig. 7. Effects of the selective ET_A antagonist BQ-123 on the LV intact muscle strips of sham ($n = 7$), MCT ($n = 7$), and MCT+bosentan rats ($n = 6$). Results are presented as percent Δdeveloped tension after BQ-123 treatment. Sham LV muscle strips showed a negative inotropic effect ($P = 0.032$, as evaluated with paired t-test), whereas the tension developed by MCT and MCT+bosentan muscle strips was unaffected ($P = 0.005$, as evaluated with one-way ANOVA).

ET-1 without counterregulatory activation of BNP gene expression in the LV of MCT-treated rats, neither myocardial hypertrophy nor fibrosis was observed, underscoring the primordial role of overload on their development (17).

Opposite to BNP and ACE, ET-1 gene expression and peptide production were similar in the RV and LV of MCT-treated rats. Several explanations can be advanced to substantiate the magnitude of LV production of ET-1. First, neurohumoral activation typically accompanies unloading (21), but because neither the LV filling pressures nor LVEDD of MCT-treated rats were lowered and their LV were atrophic, we believe unloading cannot fully explain ET-1 upregulation. Second, some degree of hypoxemia also was acknowledged in MCT-treated rats (23, 37); hence, we studied the mRNA levels of HIF-1α, a central marker of hypoxia-induced ET-1 expression, (15) having observed no differences among groups. Third, various circulating mediators (2, 24) and the sympathetic nervous system (31) are likely inducers of ET-1 gene expression in MCT-treated rats, although their influence would be expected to take place earlier in the development of PH (18). Finally, because ET-1 is an autocrine/paracrine factor in angiotensin II-induced hypertrophy (6, 12), we must point out the possibility that angiotensin II generated by the overactive ACE may contribute to ET-1 activation.

MCT animals presented significant reductions of both LVSP and heart rate. This has been interpreted previously as consequence of continuous severe sickness (24). Tachycardia would be expected as a reflex response to a lower blood pressure, but MCT-treated rats presented an impaired response to the sympathetic nervous system as manifested by reductions of β-adrenoceptor and norepinephrine neuronal transporter densities and of norepinephrine neuronal transporter and G protein-coupled receptor kinase activity (18).

Reduction of LVSP in MCT-treated rats was accompanied by disturbed hemodynamic contractility and relaxation indexes, as previously described (14). Albeit, LV fibrosis and atrophy were ruled out, and even though invasive hemodynamic indexes were obtained with a widely open pericardium, thus reducing ventricular interdependence (33), the majority of studies carried out in PH patients (22, 29) attribute LV dysfunction fundamentally to ventricular interdependence and impaired LV filling (22) or geometric modifications (4). This is supported by the development of septal hypertrophy in our group of MCT-treated rats but not by the evidence of unaltered LVEDP and LVEDD. Likewise, conserved LV volumes have been reported despite LV functional deterioration in PH (7). However, it should be stressed that because we evaluated LV dimensions through a simple septal-lateral diameter, which does not allow a thorough evaluation of LV volume, and therefore an accurate determination of LV preload, preload-dependent indexes such as dP/dt_{max} and peak isovolumetric pressures are insufficient to definitely establish impaired contractility.

To further elucidate the myocardial contractile phenotype of the LV in MCT-treated rats, safeguarding the possibility that our findings were not due to ventricular interdependence, we conducted experiments with LV myocardium on intact muscle strip preparations. The FFR is an important intrinsic regulatory mechanism of cardiac contractility; normal myocardium increases developed force with higher frequencies of stimulation over the frequency range close to the physiological heart rate, showing normal contractile reserve, but failing or dysfunctional myocardium loses this reserve, and therefore FFRs are excellent indicators for evaluating the severity of cardiac contractile dysfunction and cardiac reserve capacity as well as for the evaluation of the effectiveness of therapeutic agents in congestive HF (5). The normal myocardium from sham rat LV muscle strips presented positive FFR as expected (5, 16), whereas the muscle strips from the LV of MCT-treated rats showed overall negative FFR indicative of reduced contractile reserve (5), resembling the hypertrophied RVs of MCT-treated rats in earlier stages of PH (16, 34).

The strong local activation of ET-1 in the LV of MCT-treated rats could straightforwardly lead one to presume that this peptide might be partly underlying the disturbed contractile properties of MCT LV myocardium. Chronic effects of ET-1 have been previously studied. ET-1 administration augments basal force of contraction, prolongs relaxation, and significantly blunts responses to Ca^{2+} and isoprenaline (38). In the present study, negative FFRs were observed in the ET-1-overexpressing LV myocardium of MCT rats. Chronic ET-1 overactivity in heart disease has been associated with slower relaxation and impaired contractility through dysfunctional Ca^{2+} homeostasis and myosin heavy chain (MHC) isoform switch (10, 13, 26, 28). Curiously, the LV of rats with PH induced by either MCT (11) or hypoxia (32) undergoes MHC isoform switch, whereas ET_A receptor antagonists have noticeably been reported to partly prevent this switch in MCT RV myocardium (10). The acute effects of ET_A blockade were studied in vitro to ascertain whether there was a functional change in the acute myocardial effects of endogenous ET-1. We had previously reported a negative inotropic effect of the selective ET_A antagonist BQ-123, per se, on undissected rabbit RV papillary muscles with intact endothelium in vitro (19).

This also was observed in the present study in sham muscle strips. The contractility of LV muscle strips from MCT-treated rats, on the contrary, was unaffected by acute in vitro exposure to BQ-123, which might denote an abnormal functioning of the overactive endothelin system compared with the normal myocardium. Chronic therapy with bosentan did not restore the normal effects of BQ-123 on muscle strips of LV myocardium, but it restored the positivity of FFR compared with MCT-injected PH rats without subsequent treatment with bosentan. Indeed, although bosentan blunted MCT-induced PH as previously reported (9), reducing RV hypertrophy with concomitant attenuation of local neuroendocrine gene expression, the marked change in FFR in the LV of MCT-injected rat myocardium after chronic therapy with bosentan favors the hypothesis of a direct action of chronic ET-1 antagonism on the molecular and functional LV myocardial phenotype. Overall, these results suggest that the beneficial effects of chronic endothelin antagonism in MCT-treated rats (14) may not be dependent exclusively on attenuated PH and improved pulmonary blood flow but also on the myocardial effects of chronic ET-1 blockade.

Despite the similarities with human PH (25), given that MCT-induced PH has no human equivalent, any implication in human pathophysiology is limited. Nevertheless, we must point out that LV myocardial abnormalities may partly underlie LV dysfunction in patients with severe PH (36). Indeed, in patients with PH, normal LV filling is only restored 1 yr after single-lung transplantation even if LV geometry and RV function are immediately restored (36), and combined heart-lung transplantation is favored if severe impairment of LV function is also present because the LV may not recover after transplantation of the lungs alone (27). A patient with severely diminished LV function, however, tolerated double-lung transplantation and fully recovered cardiac function after therapy with bosentan. The authors wisely attributed this to a reduction in ventricular interaction but also admitted that bosentan might have acted directly on the myocardium (1).

In conclusion, MCT-treated rats with severe long-standing PH develop local autocrine/paracrine system activation that is not restricted to the overloaded ventricle. The LV myocardium expresses high levels of genes involved in autocrine/paracrine systems, but despite this, it does not undergo hypertrophy or fibrosis. The LV contractile phenotype, however, is altered: LV muscle strips from MCT-treated rats present negative FFR. Acute ET_A antagonism in vitro has distinct effects on contractile performance compared with sham myocardium, and chronic ET-1 blockade after MCT injection restores the positivity of LV myocardium FFR, suggesting a possible direct detrimental action of ET-1 overexpression in the LV myocardium of PH rats.

ACKNOWLEDGMENTS

We thank the excellent experimental collaboration of Daniel Gonçalves and Antónia Teles, the comments and suggestions of Marc Iglarz of Actelion Pharmaceuticals, and Actelion Pharmaceuticals for the kind gift of bosentan.

GRANTS

This work was supported by grants from Fundação para Ciência e Tecnologia (POCI/CBO/47519/2002 and POCI/SAU-MMO/47519/2004; partially funded by FEDER) and from Cardiovascular R&D Unit (51/94-FCT, Portugal).

REFERENCES

1. **Brauchlin AE, Soccal PM, Rochat T, Spiliopoulos A, Nicod LP, and Trindade PT.** Severe left ventricular dysfunction secondary to primary pulmonary hypertension: Bridging therapy with bosentan before lung transplantation. *J Heart Lung Transplant* 24: 777–780, 2005.
2. **Brunner F.** Cardiac endothelin and big endothelin in right-heart hypertrophy due to monocrotaline-induced pulmonary hypertension in rat. *Cardiovasc Res* 44: 197–206, 1999.
3. **Correia-Pinto J, Henriques-Coelho T, Oliveira SM, and Leite-Moreira AF.** Distinct load dependence of relaxation rate and diastolic function in *Oryctolagus cuniculus* and *Ratus norvegicus*. *J Comp Physiol [B]* 173: 401–407, 2003.
4. **Dong SJ, Crawley AP, MacGregor JH, Petrank YF, Bergman DW, Belenkie I, Smith ER, Tyberg JV, and Beyar R.** Regional left ventricular systolic function in relation to the cavity geometry in patients with chronic right ventricular pressure overload. *Circulation* 91: 2359–2370, 1995.
5. **Endoh M.** Force-frequency relationship in intact mammalian ventricular myocardium: physiological and pathophysiological relevance. *Eur J Pharmacol* 500: 73–86, 2004.
6. **Fujisaki H, Ito H, Hirata Y, Tanaka M, Hata M, Lin M, Adachi S, Akimoto H, Marumo F, and Hiroe M.** Natriuretic peptides inhibit angiotensin II-induced proliferation of rat cardiac fibroblasts by blocking endothelin-1 gene expression. *J Clin Invest* 96: 1059–1065, 1995.
7. **Gomez A, Unruh H, and Mink S.** Left ventricular systolic performance is depressed in chronic pulmonary emphysema in dogs. *Am J Physiol Heart Circ Physiol* 267: H232–H247, 1994.
8. **Henriques-Coelho T, Correia-Pinto J, Roncon-Albuquerque R Jr, Baptista MJ, Lourenço AP, Oliveira SM, Brandão-Nogueira A, Teles A, Fortunato JM, and Leite-Moreira AF.** Endogenous production of ghrelin and beneficial effects of its exogenous administration in monocrotaline-induced pulmonary hypertension. *Am J Physiol Heart Circ Physiol* 287: H2885–H2890, 2004.
9. **Hill NS, Warburton RR, Pietras L, and Klinger JR.** Nonspecific endothelin-receptor antagonist blunts monocrotaline-induced pulmonary hypertension in rats. *J Appl Physiol* 83: 1209–1215, 1997.
10. **Ichikawa KI, Hidai C, Okuda C, Kimata SI, Matsuoka R, Hosoda S, Quertermous T, and Kawana M.** Endogenous endothelin-1 mediates cardiac hypertrophy and switching of myosin heavy chain gene expression in rat ventricular myocardium. *J Am Coll Cardiol* 27: 1286–1291, 1996.
11. **Ishikawa S, Honda M, Yamada S, Goto Y, Morioka S, Ishinaga Y, Murakami Y, Masumura S, and Moriyama K.** Different biventricular remodeling of myosin and collagen in pulmonary hypertension. *Clin Exp Pharmacol Physiol* 19: 723–732, 1992.
12. **Ito H, Hirata Y, Adachi S, Tanaka M, Tsujino M, Koike A, Nogami A, Murumo F, and Hiroe M.** Endothelin-1 is an autocrine/paracrine factor in the mechanism of angiotensin II-induced hypertrophy in cultured rat cardiomyocytes. *J Clin Invest* 92: 398–403, 1993.
13. **Iwanaga Y, Kihara Y, Hasegawa K, Inagaki K, Yoneda T, Kaburagi S, Araki M, and Sasayama S.** Cardiac endothelin-1 plays a critical role in the functional deterioration of left ventricles during the transition from compensatory hypertrophy to congestive heart failure in salt-sensitive hypertensive rats. *Circulation* 98: 2065–2073, 1998.
14. **Jasmin JF, Lucas M, Cernacek P, and Dupuis J.** Effectiveness of a nonselective $ET_{A/B}$ and a selective ET_A antagonist in rats with monocrotaline-induced pulmonary hypertension. *Circulation* 103: 314–318, 2001.
15. **Kakinuma Y, Miyauchi T, Yuki K, Murakoshi N, Goto K, and Yamaguchi I.** Novel molecular mechanism of increased myocardial endothelin-1 expression in the failing heart involving the transcriptional factor hypoxia-inducible factor-1α induced for impaired myocardial energy metabolism. *Circulation* 103: 2387–2394, 2001.
16. **Kögler H, Hartmann O, Leineweber K, Nguyen van P, Schott P, Brodde OE, and Hasenfuss G.** Mechanical load-dependent regulation of gene expression in monocrotaline-induced right ventricular hypertrophy in the rat. *Circ Res* 93: 230–237, 2003.
17. **Koide M, Carabello BA, Conrad CC, Buckley JM, DeFreyte G, Barnes M, Tomanek RJ, Wei CC, Dell'Italia LJ, Cooper GIV, and Zile MR.** Hypertrophic response to hemodynamic overload: role of load vs. renin-angiotensin system activation. *Am J Physiol Heart Circ Physiol* 276: H350–H358, 1999.
18. **Leineweber K, Brandt K, Wludyka B, Beilfuβ A, Pönicke K, Heinroth-Hoffmann I, and Brodde OE.** Ventricular hypertrophy plus neuro-

humoral activation is necessary to alter the cardiac β-adrenoceptor system in experimental heart failure. *Circ Res* 91: 1056–1062, 2002.

19. **Leite-Moreira AF and Brás-Silva C.** Inotropic effects of ET_B receptor stimulation and their modulation by endocardial endothelium, NO, and prostaglandins. *Am J Physiol Heart Circ Physiol* 287: H1194–H1199, 2004.
20. **Leite-Moreira AF and Correia-Pinto J.** Load as an acute determinant of end-diastolic pressure-volume relation. *Am J Physiol Heart Circ Physiol* 280: H51–H59, 2001.
21. **Lisy O, Redfield MM, Jovanovic S, Jougasaki M, Jovanovic A, Leskinen H, Terzic A, and Burnett JC Jr.** Mechanical unloading versus neurohumoral stimulation on myocardial structure and endocrine function In vivo. *Circulation* 102: 338–343, 2000.
22. **Menzel T, Wagner S, Kramm T, Mohr-Kahaly S, Mayer E, Braeuninger S, and Meyer J.** Pathophysiology of impaired right and left ventricular function in chronic embolic pulmonary hypertension. Changes after pulmonary thromboendarterectomy. *Chest* 118: 897–903, 2000.
23. **Meyrick B, Gamble W, and Reid L.** Development of *Crotalaria* pulmonary hypertension: hemodynamic and structural study. *Am J Physiol Heart Circ Physiol* 239: H692–H702, 1980.
24. **Miyauchi T, Yorikane R, Sakai S, Sakurai T, Okada M, Nishikibe M, Yano M, Yamaguchi I, Sugishita Y, and Goto K.** Contribution of endogenous endothelin-1 to the progression of cardiopulmonary alterations in rats with monocrotaline-induced pulmonary hypertension. *Circ Res* 73: 887–897, 1993.
25. **Molteni A, Ward WF, Ts'ao CH, Port CD, and Solliday NH.** Monocrotaline-induced pulmonary endothelial dysfunction in rats. *Proc Soc Exp Biol Med* 176: 88–94, 1984.
26. **Onishi K, Ohno M, Little WC, and Cheng CP.** Endogenous endothelin-1 depresses left ventricular systolic and diastolic performance in congestive heart failure. *J Pharmacol Exp Ther* 288: 1214–1222, 1999.
27. **Pielsticker EJ, Martinez FJ, and Rubenfire M.** Lung and heart-lung transplant practice patterns in pulmonary hypertension centers. *J Heart Lung Transplant* 20: 1297–1304, 2001.
28. **Rothermund L, Pinto YM, Hocher B, Vetter R, Leggewie S, KoEmehl P, Orzechowski HD, Kreutz R, and Paul M.** Cardiac endothelin system impairs left ventricular function in renin-dependent hypertension via decreased sarcoplasmic reticulum Ca^{2+} uptake. *Circulation* 102: 1582–1588, 2000.
29. **Schena M, Clini E, Errera D, and Quadri A.** Echo-Doppler evaluation of left ventricular impairment in chronic cor pulmonale. *Chest* 109: 1446–1451, 1996.
30. **Schott P, Singer SS, Kögler H, Neddermeier D, Leineweber K, Brodde OE, Regitz-Zagrosek V, Schmidt B, Dihazi H, and Hasenfuss G.** Pressure overload and neurohumoral activation differentially affect the myocardial proteome. *Proteomics* 5: 1372–1381, 2005.
31. **Seyfarth T, Gerbershagen HP, Giessler C, Leineweber K, Heinroth-Hoffman I, Pönicke K, and Brodde OE.** The cardiac β-adrenoceptor-G-protein(s)-adenylyl cyclase system in monocrotaline treated rats. *J Mol Cell Cardiol* 32: 2315–2326, 2000.
32. **Sharma S, Taegtmeyer H, Adrogue J, Razeghi P, Sen S, Ngumbela K, and Essop MF.** Dynamic changes of gene expression in hypoxia-induced right ventricular hypertrophy. *Am J Physiol Heart Circ Physiol* 286: H1185–H1192, 2004.
33. **Slinker BA and Glantz SA.** End-systolic and end-diastolic ventricular interaction. *Am J Physiol Heart Circ Physiol* 251: H1062–H1075, 1986.
34. **Versluis JP, Heslinga JW, Sipkema P, and Westerhof N.** Contractile reserve but not tension is reduced in monocrotaline-induced right ventricular hypertrophy. *Am J Physiol Heart Circ Physiol* 286: H979–H984, 2004.
35. **Werchan PM, Summer WR, Gerdes AM, and McDonough KM.** Right ventricular performance after monocrotaline-induced pulmonary hypertension. *Am J Physiol Heart Circ Physiol* 256: H1328–H1336, 1989.
36. **Xie GY, Lin CS, Preston HM, Taylor CG, Kearney K, Sapin PM, and Smith MD.** Assessment of left ventricular diastolic function after single lung transplantation in patients with severe pulmonary hypertension. *Chest* 114: 477–481, 1998.
37. **Yuyama H, Fujimori A, Sanagi M, Koakutsu A, Sudoh K, Sasamata M, and Miyata K.** The orally active nonpeptide selective endothelin ET_A receptor antagonist YM598 prevents and reverses the development of pulmonary hypertension in monocrotaline-treated rats. *Eur J Pharmacol* 496: 129–139, 2004.
38. **Zolk O, Munzel F, and Eschenhagen T.** Effects of chronic endothelin-1 stimulation on cardiac myocyte contractile function. *Am J Physiol Heart Circ Physiol* 286: H1248–H1257, 2004.